

host–guest interactions in the present research will serve us to consistently understand the structure–activity relationship in peptide-based molecular assemblies.

The synthetic route, compound characterization, and proton assignments for guest molecule BP-FF are shown in the Supporting Information (Scheme S1, Figures S1–S4). Possessing two positively charged pyridinium sites and a hydrophobic aromatic skeleton, BP-FF can be readily encapsulated in the cavity of various macrocyclic receptors through multiple host–guest interactions: 1) BP can form stable inclusion complexes with CBs, in which the main driving force was ascribable to ion-dipole interaction between the positive charges of the bipyridinium salts and the portal oxygen atoms of CBs;^[7] 2) WP5A was found to form 1:1 binary inclusion complex with BP mainly through electrostatic interaction;^[8] and 3) more remarkably, tetrasulfonated 1,5-dinaphtho-32-crown-8 (DNC), a new type of water-soluble crown ether developed in our group, can form a highly stable charge-transfer complex with BP through favorable electrostatic and π -stacking interactions.^[9] In our case, after validating the 1:1 complex stoichiometry by Job plots and mass spectrometry (Supporting Information, Figures S5–S12), the binding constants (K_s) in the complexation of BP-FF with CB[7], CB[8], WP5A, and DNC were determined as 5.33×10^4 , 8.08×10^4 , 8.20×10^4 , and $7.94 \times 10^6 \text{ M}^{-1}$, respectively (Supporting Information, Figures S13–S16).

The binding modes between BP-FF and four macrocycles were further investigated by ^1H NMR and UV/Vis spectroscopy experiments. In BP-FF/CB[7] complex, the protons ($\text{H}_{\text{b,c}}$) of the pyridinium moiety in BP-FF exhibited a large upfield shift in the presence of CB[7], while those of the phenyl rings were essentially unchanged (Figure 1 b,c). Therefore, we can speculate that pyridinium moiety was tightly bound to CB[7], leaving the diphenylalanine moiety outside the cavity. In BP-FF/CB[8] complex, both pyridinium ($\text{H}_{\text{a,b,c}}$ in Figure 1 d) and partial phenyl protons shifted to higher field upon addition of equivalent amount of CB[8], indicating that the pyridinium moiety and phenyl ring of diphenylalanine were concurrently included in the cavity of CB[8]. Furthermore, the ^1H – ^1H COSY spectrum showed that the pyridinium next to N-terminus ($\text{H}_{\text{a,b}}$) underwent a pronounced upfield shifts by CB[8] (Supporting Information, Figure S17). Considering the peptide sequence recognition with CBs,^[10] the benzene ring next to N-terminus should be priority to be included in the cavity of CB[8] because of the unfavorable repulsion between carboxyl group at C-terminus and the portal oxygen atoms of CBs. The coexistence of phenyl and bipyridinium moieties in the cavity of CB[8] was further indicated by the broad absorption at long-wavelength region in UV/Vis spectra, indicative of the formation of charge-transfer interaction in BP-FF/CB[8] complex (Supporting Information, Figure S18, red line).

As shown in Figure 1 f, when an equimolar amount of WP5A was added, the proton peaks of the pyridinium ring of BP-FF underwent an upfield shift. A ROESY spectrum of BP-FF/WP5A complex also showed the obvious correlation peaks between pyridinium protons and the aromatic protons of WP5A (Supporting Information, Figure S19). These phenomena jointly demonstrate the host–guest association

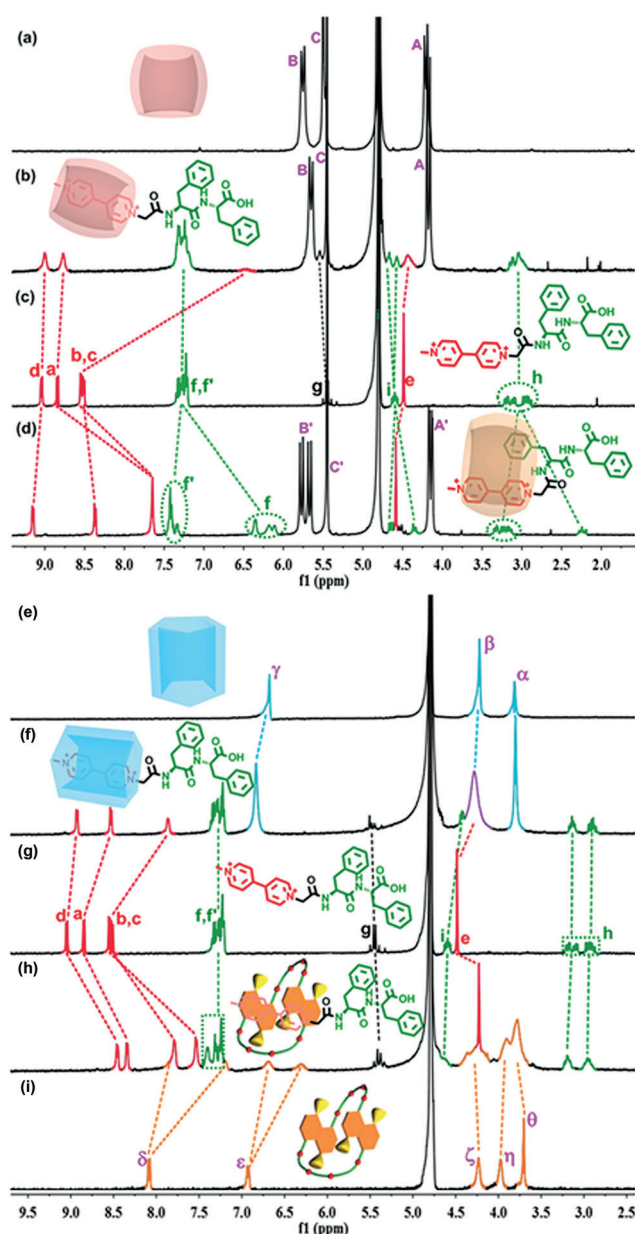


Figure 1. ^1H NMR spectra (400 MHz, D_2O) of a) free CB[7], b) BP-FF/CB[7] complex, c) free BP-FF, d) BP-FF/CB[8] complex, e) free WP5A, f) BP-FF/WP5A complex, g) free BP-FF, h) BP-FF/DNC complex, and i) free DNC at 25 °C ([BP-FF] = [CB[7]] = [CB[8]] = [WP5A] = [DNC] = 2.0 mM).

between WP5A and BP-FF in water. Meanwhile, considering the numerous alkoxybenzene moieties in WP5A as strong electron-rich groups, the broad absorption band centered at 450 nm could be contributed to the charge-transfer interaction with the electron-deficient BP-FF in water (Supporting Information, Figure S18, green line). Finally, as can be seen from Figure 1 h, the chemical shifts of aromatic protons in DNC and all protons in bipyridinium moiety of BP-FF exhibited an upfield shift upon complexation with each other, which are mainly attributed to mutual shielding effect between naphthalene and pyridinium rings. Similarly, a new

absorption band centered at 460 nm was observed upon mixing DNC and BP-FF in aqueous solution (Supporting Information, Figure S18, purple line), here again indicating that bipyridinium part was encapsulated between two naphthyl rings of DNC through π -stacking interaction (Supporting Information, Figure S20). Overall, ^1H NMR and UV/Vis spectra jointly demonstrate that in our case, despite the different molecular shape, cavity size, and charge number, four macrocycles can exclusively entrap the bipyridinium moiety of BP-FF through multiple noncovalent forces, namely, the ion-dipole interconnection with CB[7] and CB[8], the charge-transfer interaction in CB[8], WP5A, and DNC, and the electrostatic attraction with WP5A and DNC. Thus, it is believed that the highly affiliative host-guest complexation may have a great impact on the topological morphology of FF self-aggregates, and this hypothesis would be validated by the microscopic investigation, as described below.

Transmission electron microscopy (TEM) and scanning electron microscopy (SEM) were used to investigate the influence of hosts on the self-assembled structures of BP-FF. As shown in Figure 2 a,b, fine nanofibers with 20 nm diameter were formed by BP-FF alone. Interestingly, diverse self-

assembled nanostructures were obtained by mixing BP-FF with equimolar macrocyclic hosts in aqueous solution. In the case of BP-FF \subset CB[7] complex, a number of nanorods were observed with the length and width of about 500 and 200 nm, respectively (Figure 2 c,d). Meanwhile, DLS data showed that the assembly of BP-FF \subset CB[7] complex possessed an average hydrodynamic diameter of 672 nm in solution (Supporting Information, Figure S21). Moreover, the octahedron-like structures at the micrometer scale were observed for the BP-FF \subset CB[8] complex, which is rarely reported in the FF-related nanosystems (Figure 2 e,f). TEM images of self-assembled BP-FF \subset WP5A complex showed right-handed helical nanowires with the diameters around 600 nm (Figure 2 h). More notably, left-handed helical nanowires were exclusively found in SEM images (Figure 2 g). This opposite helicity in BP-FF \subset WP5A complex is probably attributed to the different binding mode and affinity of extensive carboxyl groups in WP5A with the sample matrix (that is, carbon film in TEM and silicon wafer in SEM experiments, respectively). Furthermore, rectangular nanosheets were found in the BP-FF \subset DNC complex, with the length ranging from 200 to 700 nm (Figure 2 i,j). These microscopic investigation results demonstrate that the addition of macrocyclic compounds can dramatically influence the spatial alignment of FF and then induce a broad range of morphological variation from nanofibers to nanorods, octahedron-like nanostructure, helical nanowires, and rectangular nanosheets. Interestingly, the addition of CB[8] or DNC as competitive host to the BP-FF \subset CB[7] and BP-FF \subset WP5A assemblies could also trigger the supramolecular structural changes (Supporting Information, Figures S22). These microscopic investigation results further corroborated the K_s -dependent molecular assembling behaviors.

Circular dichroism (CD) and Fourier transform IR (FTIR) spectroscopy were used to investigate the spatial orientation of BP-FF and its host-guest complexes (Supporting Information, Figures S23 and S24). The CD signature of BP-FF nanofiber was characterized by a strong positive band at 198 nm (π - π^* transition), corresponding to the assumed β -turns of FF in solution.^[11] Despite the signal intensity was a little weakened as compared to the parent BP-FF, similar CD spectral features were observed for the BP-FF \subset CB[7] and BP-FF \subset WP5A complexes, implying that the introduction of exogenous CB[7] and WP5A could not affect the main assembling mode of FF moiety. This speculation was further supported by FTIR spectroscopy, that is, two characteristic peaks were clearly observed at 1640 and 1680 cm^{-1} in both free BP-FF and BP-FF \subset CB[7] assembly, which could be assigned to the β -turn conformation of FF backbone.^[11] In the BP-FF \subset DNC complex, besides the peak assignment on β -turn conformation at 195 nm, the negative band at 233 nm and positive band at 249 nm were contributed to the induced CD signals from DNC's naphthyl rings. Meanwhile, the peaks at 1639 and 1683 cm^{-1} in FTIR spectrum further verified the β -turn conformation, which was consistent with the CD results.

In contrast, an obvious spectral change was observed in the CD spectrum of BP-FF \subset CB[8] complex, in which the negative peaks at 193 nm could be assigned to the formation

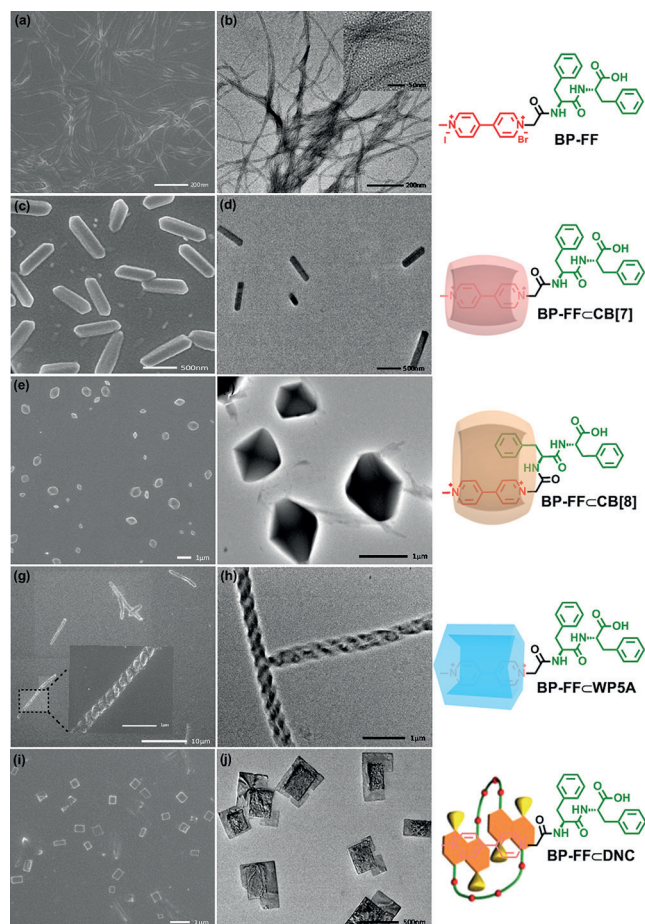


Figure 2. a), c), e), g), i) SEM and b), d), f), h), j) TEM images of the self-assembly of a), b) free BP-FF, c), d) BP-FF \subset CB[7] complex, e), f) BP-FF \subset CB[8] complex, g), h) BP-FF \subset WP5A complex, and i), j) BP-FF \subset DNC complex ([BP-FF] = [CB[7]] = [CB[8]] = [WP5A] = [DNC] = 0.02 mM, pH 6.0, 25 °C).

of β -sheet structure in the molecular assembling process.^[12] Combining the aforementioned ^1H NMR spectroscopic results, we can infer that the unique CD spectroscopic behaviors were mainly attributed to the coexistence of bipyridinium and phenyl rings in the cavity of CB[8]. Overall, these spectroscopic results jointly demonstrate that FF residue can predominantly maintain its β -turn conformation in the BP-FF \subset CB[7], BP-FF \subset WP5A, and BP-FF \subset DNC complexes, while the charge-transfer interaction between bipyridinium and phenyl moieties upon complexation with CB[8] can profoundly change the assembling mode of BP-FF, thus leading to a β -sheet conformation in solution and an octahedron-like structures in the solid state.

Furthermore, the formation of a charge-transfer complex between bipyridinium and phenyl moieties in the BP-FF \subset CB[8] complex inspired us to hypothesize that a reversible binding process may be achieved by introducing an appropriate guest. Therefore, azophenyl imidazolium salt (Azoim) was chosen as the competitive guest to expel the phenyl group of FF from the cavity of CB[8], taking the good electron-donating properties and photoinduced isomerization ability of azobenzene units into account. ^1H NMR experiments were carried out to investigate the molecular binding behaviors in the ternary Azoim·BP-FF \subset CB[8] complex (Supporting Information, Figures S25 and S26). As shown in Figure S25, the phenyl protons at 6.25 ppm in FF exhibited no obvious change upon addition of Azoim into BP-FF \subset CB[8] complex, suggesting that the phenyl ring could not be expelled by Azoim. However, considering that both of the pyridinium ($\text{H}_{\text{c,d}}$) and Azoim protons gave a sizable upfield shift, we can infer that part of azophenyl group in Azoim was readily accommodated by CB[8] to form a ternary complex, and the imidazolium moiety was located outside the cavity to avoid unfavorable electrostatic repulsion with bipyridinium group. Meanwhile, the negative bands at 199 and 210 nm in CD spectra indicated a β -sheet structure in solution,^[12] which was similar to the assembling mode in BP-FF \subset CB[8] complex. Moreover, the enhanced CD signal intensity of Azoim at about 340 nm further corroborated the partial inclusion of Azoim in the BP-FF \subset CB[8] complex (Supporting Information, Figure S27, blue line), as illustrated in Scheme 2.

Interestingly, when the Azoim·BP-FF \subset CB[8] complex was exposed to UV irradiation, only BP-FF could be kept in solution, accompanied by the precipitation of Azoim \subset CB[8] complex from the solution (Supporting Information, Fig-

ure S28). Along with the spectroscopic investigation in aqueous solution, there was an obvious morphological change in the solid state; that is, well-defined rhombic dodecahedrons were observed upon complexation of CB[8] with BP-FF and *trans*-Azoim (Figure 3), while it was gradually transformed to nanofibers under sufficient UV light irradiation. Comparatively, in the control experiment, Azoim \subset CB[8] complex only formed nanoparticles upon irradiation with UV light (Supporting Information, Figure S29).

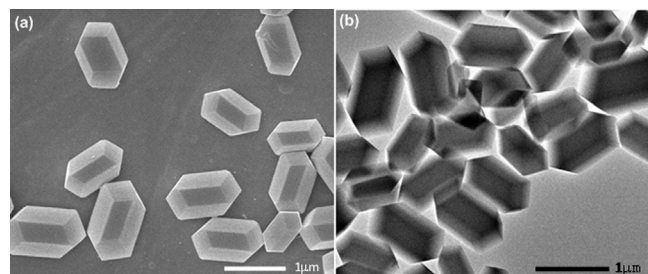


Figure 3. a) SEM and b) TEM images of the rhombohedral dodecahedrons formed by Azoim·BP-FF \subset CB[8] complex ([Azoim] = [BP-FF] = [CB[8]] = 0.02 mM, pH 6.0, 25 °C).

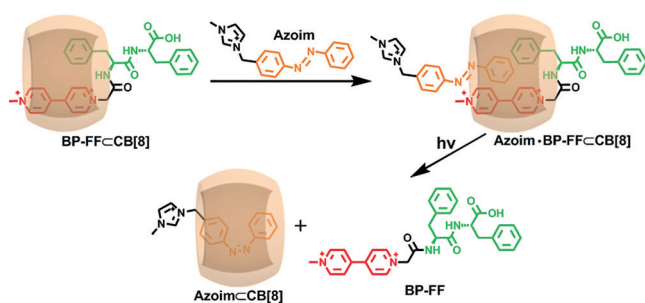
In conclusion, we put forward a supramolecular modulation method to efficiently control the assembling morphology of FF backbone simply through host-guest interactions. Superior to the previous FF-based nanostructures, the complexation of BP-FF with different water-soluble macrocyclic receptors (namely, CB[7], CB[8], WP5A, and DNC) could conveniently fabricate diverse morphologically interesting aggregates, including nanorods, octahedron-like nanostructure, helical nanowires, and rectangular nanosheets, without necessitating any chemical modification. The noncovalent association of bioactive molecules with artificial macrocycles in the present work further stress the distinct advantage of supramolecular cooperativity in the design and engineering of biomimetic and multistimuli-responsive hybrid molecular assemblies, and thus we expect that the obtained supramolecular aggregates can provide us with a facile modular strategy for the creation of more advanced biocompatible materials with new functionality.

Acknowledgements

We thank the National Natural Science Foundation of China (Nos. 21432004, 21472100, and 91527301) for financial support.

Keywords: diphenylalanine · host-guest complexes · macrocyclic receptors · molecular recognition · supramolecular assembly

How to cite: *Angew. Chem. Int. Ed.* **2016**, 55, 11452–11456
Angew. Chem. **2016**, 128, 11624–11628



Scheme 2. Photoregulation process of the BP-FF \subset CB[8] complex in the presence of Azoim.

- [1] a) Y. Suzuki, M. Endo, H. Sugiyama, *Nat. Commun.* **2015**, *6*, 8052; b) E. Gazit, *Chem. Soc. Rev.* **2007**, *36*, 1263–1269; c) Z. G. Wang, B. Ding, *Acc. Chem. Res.* **2014**, *47*, 1654–1662; d) M. Langecker, V. Arnaut, T. G. Martin, J. List, S. Renner, M. Mayer, H. Dietz, F. C. Simmel, *Science* **2012**, *338*, 932–936.
- [2] a) A. Ray, B. Norden, *FASEB J.* **2000**, *14*, 1041–1060; b) S. B. Fonseca, M. P. Pereira, S. O. Kelley, *Adv. Drug Delivery Rev.* **2009**, *61*, 953–964; c) V. A. Kumar, N. L. Taylor, S. Shi, N. C. Wickremasinghe, R. N. D'Souza, J. D. Hartgerink, *Biomaterials* **2015**, *52*, 71.
- [3] a) W. Kim, J. Thevenot, E. Ibarboure, S. Lecommandoux, E. L. Chaikof, *Angew. Chem. Int. Ed.* **2010**, *49*, 4257–4260; *Angew. Chem.* **2010**, *122*, 4353–4356; b) R. Chapman, M. Danial, M. L. Koh, K. A. Jolliffe, S. Perrier, *Chem. Soc. Rev.* **2012**, *41*, 6023–6041; c) F. Versluis, H. R. Marsden, A. Kros, *Chem. Soc. Rev.* **2010**, *39*, 3434–3444.
- [4] a) M. Reches, E. Gazit, *Science* **2003**, *300*, 625–627; b) Q. Li, H.-C. Ma, Y. Jia, J.-B. Li, B.-H. Zhu, *Chem. Commun.* **2015**, *51*, 7219–7221; c) X.-H. Yan, P.-L. Zhu, J.-B. Li, *Chem. Soc. Rev.* **2010**, *39*, 1877–1890.
- [5] a) R.-L. Huang, W. Qi, R.-X. Su, J. Zhao, Z.-M. He, *Soft Matter* **2011**, *7*, 6418; b) Y. Su, X.-H. Yan, A.-H. Wang, J.-B. Fei, Y. Cui, Q. He, J.-B. Li, *J. Mater. Chem.* **2010**, *20*, 6734; c) M. Reches, E. Gazit, *Nat. Nanotechnol.* **2006**, *1*, 195–200.
- [6] a) Y.-F. Wang, R.-L. Huang, W. Qi, Z.-J. Wu, R.-X. Su, Z.-M. He, *Nanotechnology* **2013**, *24*, 465603; b) Y.-F. Wang, W. Qi, R.-L. Huang, X.-J. Yang, M.-F. Wang, R.-X. Su, Z.-M. He, *J. Am. Chem. Soc.* **2015**, *137*, 7869–7880.
- [7] a) H. J. Kim, W. S. Jeon, Y. H. Ko, K. Kim, *Proc. Natl. Acad. Sci. USA* **2002**, *99*, 5007–5011; b) W. S. Jeon, H. J. Kim, C. Lee, K. Kim, *Chem. Commun.* **2002**, 1828.
- [8] T. Ogoshi, M. Hashizume, T. A. Yamagishi, Y. Nakamoto, *Chem. Commun.* **2010**, *46*, 3708–3710.
- [9] L. Chen, H.-Y. Zhang, Y. Liu, *J. Org. Chem.* **2012**, *77*, 9766–9773.
- [10] M. E. Bush, N. D. Bouley, A. R. Urbach, *J. Am. Chem. Soc.* **2005**, *127*, 14511–14517.
- [11] M. Gupta, A. Bagaria, A. Mishra, P. Mathur, A. Basu, S. Ramakumar, V. S. Chauhan, *Adv. Mater.* **2007**, *19*, 858–861.
- [12] A. M. Smith, R. J. Williams, C. Tang, P. Coppo, R. F. Collins, M. L. Turner, A. Saiani, R. V. Ulijn, *Adv. Mater.* **2008**, *20*, 37–41.

Received: June 3, 2016

Published online: August 16, 2016